Scale-Model Tests of Airfoils in Simulated Heavy Rain

E. C. Hastings Jr.* and G. S. Manuel*
NASA Langley Research Center, Hampton, Virginia

This paper discusses some of the surface water characteristics obtained in simulated heavy rain experiments conducted at the NASA Langley Research Center. The objective was to measure water film distributions and discrete film thicknesses on several two-dimensional model wings. The water film distributions on the upper surfaces are shown in photographs taken from cameras mounted above the models; the film thickness data were obtained using resistance sensors mounted flush with the upper and lower wing model surfaces. It was observed that two different clean wing models developed similar water film patterns consisting of a continuous sheet that extended to midchord and broke off in runoff streams. The water film pattern on the flapped model differed from the clean wing configuration. On the upper surface of the flapped model, the continuous sheet was thinner and a great deal of water was observed in and around the flap gaps.

Nomenclature

c = chord length of model wing
LWC = liquid water content
R_c = Reynolds number, based on chord length
RR_e = equivalent rainfall rate
V = velocity
x = distance aft of wing leading edge
α = angle of attack of wing
δ = boundary-layer thickness
δ_f = thickness of water film on surface
θ = pitch attitude of model wing

Introduction

RESEARCH is currently being conducted at the National Aeronautics and Space Administration (NASA) and other agencies to investigate the effects of heavy rain on aircraft performance. An important part of this research is the effect of water collected on the wing surface. In addition to adding weight, the water acts as a surface contaminant that may influence pressure gradients, skin-friction drag, and boundary-layer characteristics and transition. All of these factors can influence lift and/or drag. This paper discusses some of the recent results from experimental research being conducted at the Langley Research Center on surface water characteristics and effects.

Data from simulated heavy rain tests with models of clean and flapped wings. Flow patterns on the model surfaces were recorded with overhead cameras and film thickness measurements were obtained with nonintrusive sensors flush mounted in the wing models. The data are discussed as functions of wing configuration, angle of attack, and liquid water content. Although the data currently available do not allow a complete evaluation of surface water effects, the data are used to indicate potential sources of wing performance decrements.

Test Description

Two tests are discussed in this paper. The first[1] was conducted in a temporary flow apparatus using a model wing with a NACA 0012 section and chord length of 1 ft. The setup of test 1 is shown in Fig. 1. The diameter of the flow apparatus was 36 in. at the diffuser exit and 25 in. at the fan. The spray bar and nozzle were located about 8 ft upstream of the exit. The model wing was mounted about 1 ft upstream of the exit and extended across the entire diffuser. Because the flow angularity error in this facility is not known, these data are referenced to the wing pitch attitude θ rather than to angle of attack.

Figure 2 is a sketch of the water thickness measuring sensor developed at Langley for use in this test.[1] It consists of two metal electrodes separated by a nylon insulator. Sensors were flush mounted in the wing and measured the water thickness by measuring the resistance of the water over the electrodes.

Test 2 was conducted in the 4×7 m tunnel.[2] A photograph of the test setup is shown in Fig. 3. The test used a model wing with a NACA 64-210 section with a span of 8 ft and a chord length of 2.5 ft. This model wing could be tested either in the clean configuration or with the leading-edge slats and double-slotted trailing-edge flaps extended. A cross section of the model in the flapped configuration is shown in Fig. 4. The model wing was mounted between the end plates to provide two-dimensional flow. All instrumentation was located in the center 1 ft section of the span. This section was isolated from the outer panels by an internal strain gage balance system. A

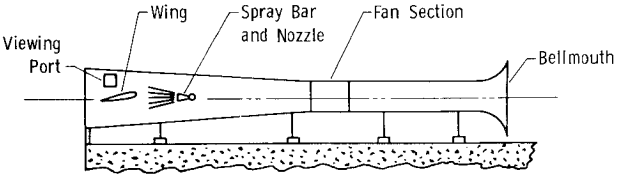

Fig. 1 Setup of test 1 in the 3 ft diam flow apparatus.

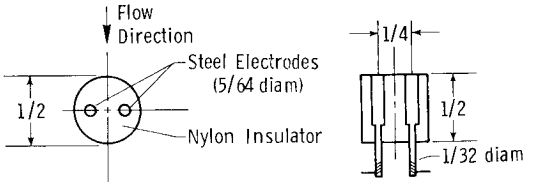

Fig. 2 Sensor used for measuring surface water thickness.

Received Dec. 4, 1984; presented as Paper 85-0259 at the 23rd Aerospace Sciences Meeting, Reno, Nev., Jan. 14-17. 1985; revision received March 8, 1985.

*Aerospace Engineer, Subsonic Aerodynamics Branch, Low-Speed Aerodynamics Division.

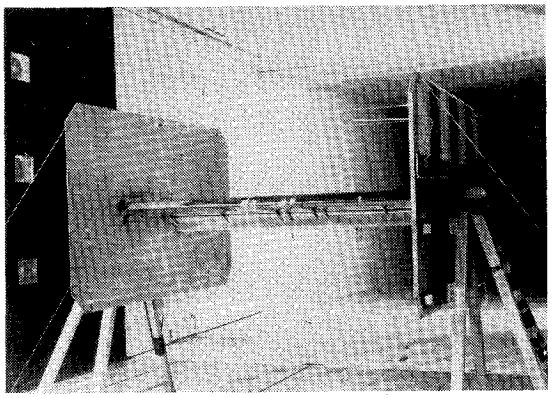

Fig. 3 Setup of test 2 in the 4×7 m tunnel.

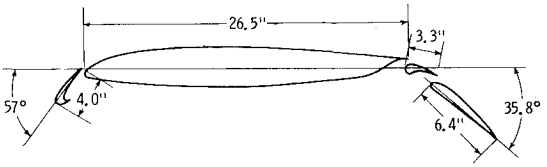

Fig. 4 Profile of model with leading-edge slats and trailing-edge flaps extended (NACA 64-210 section).

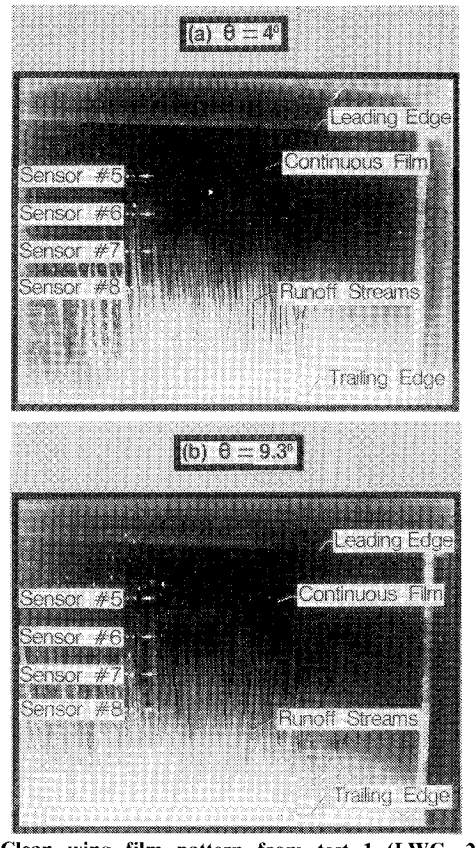

Fig. 5 Clean wing film pattern from test 1 (LWC = 20 g/m^3, $R_c = 8.9 \times 10^6$).

Table 1 Sensor locations

Test	Upper surface, x/c,%	Lower surface, x/c,%
1	16.7, 29.2, 54.2	16.7, 29.2, 41.7, 54.2
2	14.4, 20.7, 28.3, 43.2, 50.7	14.4, 28.3, 43.2, 50.7

spray bar and nozzles were located in the tunnel test section about 25 ft upstream of the model wing.

The model wings used in tests 1 and 2 were instrumented with sensors located at the midspan. The film thickness data were obtained at the chordwise stations noted in Table 1. Test conditions and water spray characteristics for both tests are given in Table 2. The equivalent rain rates RR_e were developed from measured values of liquid water content (LWC).[2] The calculated values of RR_e in Table 2 all represent extremely high rain rates, although they are considerably less than some rates measured in actual rain that exceeded 1800 mm/h.

The spray characteristics in Table 2 were obtained with shadowgraph techniques.[2] In test 1 (in which the same nozzle was used throughout), the measurements indicate that all of the droplets were of nearly uniform size in all the runs. In test 2, different spray nozzles were used to obtain more representative drop size distributions (i.e., a higher percentages of large droplets at these high values of LWC).

In test 2, data were obtained for the model wing with and without transition strips near the leading edge. Since the wing in test 1 had no strip and since the test 2 data showed that the strip made no significant difference in the results, all film thickness data in this report are given for the model wings with no transition strip.

Results and Discussion

Wings Without Flaps

Typical water film patterns on the upper surface from test 1 are shown in Fig. 5. As shown, the spray caused a smooth continuous film to form on the forward section of the surface. Aft of this location, the film broke down into many individual runoff streams, extending to the wing trailing edge. The same general pattern was observed at both $\theta = 4$ and 9.3 deg and at LWC between 13 and 35 g/m^3. Figure 6 shows typical flow pattern on the clean wing from test 2 at $\alpha = 0$ deg and LWC = 39 g/m^3. Although the conditions and airfoil sections of tests 1 and 2 are not the same, the water film patterns shown in Figs. 5 and 6 are very similar.

Water patterns on wing surfaces were also photographed during recent simulated heavy rain experiments conducted at the Massachusetts Institute of Technology.[3] Those experiments used a 1×1 ft wind tunnel to investigate simulated rain effects on models of laminar flow wings with various surface finishes. Although the airfoil shape and test Reynolds numbers differed from those of the tests reported here, photographs of the unwaxed wings also showed water film patterns similar to those in Figs. 5 and 6.

Figure 7 shows a typical flow pattern on the clean wing from test 2 at $\alpha = 14$ deg and LWC = 39 g/m^3. At this angle of at-

Table 2 Test conditions and water spray characteristics

Test 1, clean wing configuration, mean droplet diameter 0.40 mm		
V, m/s	LWC, g/m^3	RR_e, mm/h
24.7	35	1134
42.4	20	648
34.1	16	518
42.4	13	421

Test 2

	Test conditions			Spray characteristics	
				Droplet diameter, mm	
Wing configuration	V, m/s	LWC, g/m^3	RR_e, mm/h	Mean	Maximum
Clean	75.0	39	1264	0.47	1.8
Clean	63.1	31	1004	0.55	2.5
Clean	34.1	17	501	0.90	3.0
Flapped	48.5	20	648	1.00	3.8

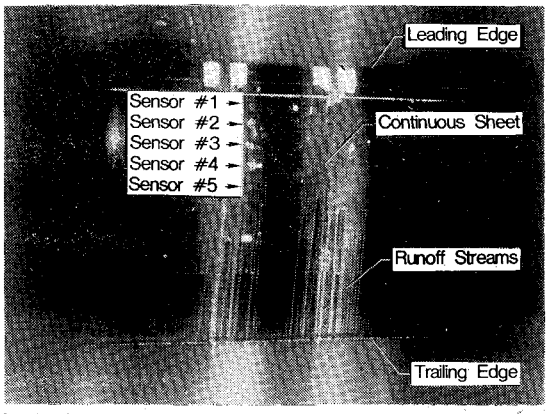

Fig. 6 Typical water film patterns on upper surface from test 2 with the clean wing at $\alpha = 0$ deg (LWC = 39 g/m^3, $R_c = 3.8 \times 10^6$).

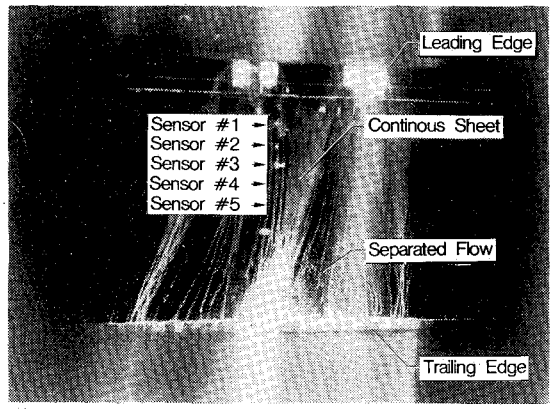

Fig. 7 Clean wing film patterns from test 2 at $\alpha = 14$ deg (LWC = 39 g/m^3, $R_c = 3.8 \times 10^6$).

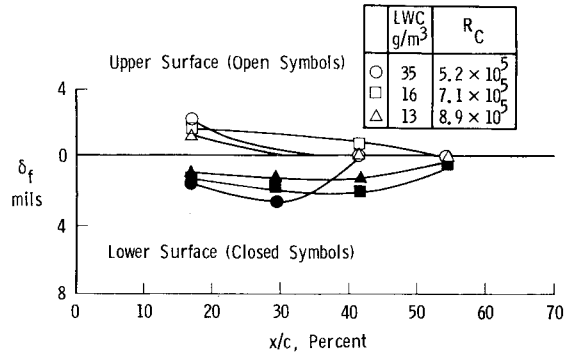

Fig. 8 Clean wing film thickness measurements from test 1 at $\theta = 4$ deg.

tack, the photographs typically showed a large region of apparently separated flow on the upper surface between breakdown of the continuous sheet and the trailing edge. This is believed to be a potential source of performance penalities and will be discussed in more detail later.

Some of the measured values of δ_f from test 1 at $\theta = 4$ deg are shown in Fig. 8. These and other data[1] indicate that the maximum thickness on the upper surface was about 2 mil at $x/c = 16.7\%$. The thickness of the continuous film decreased aft of this location before breaking down into runoff streams aft of midchord. However, the measurements on the lower surface show that the film was generally thicker on the lower surface and that the maximum thickness occurred further aft on the model. The test 1 data in Fig. 8 and other data[1] indicate

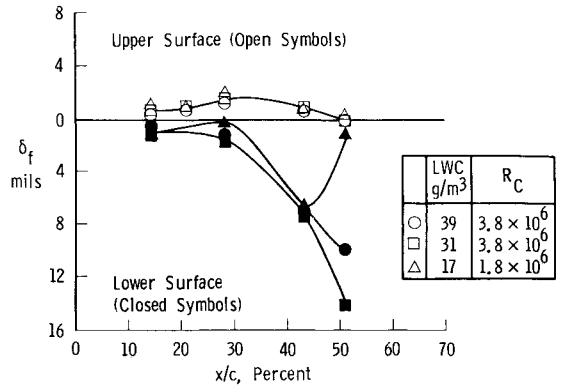

Fig. 9 Clean wing film thickness measurements from test 2 at $\alpha = 4$ deg.

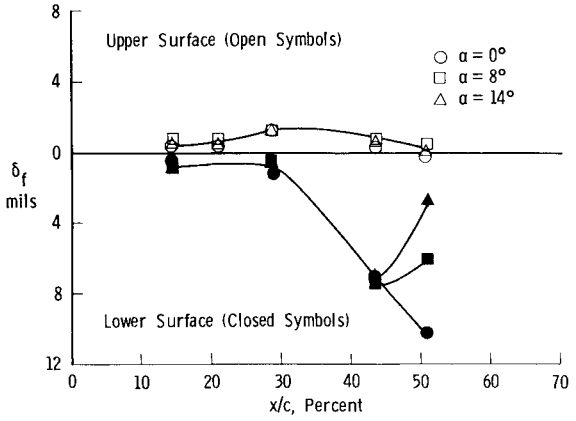

Fig. 10 Clean wing film thickness measurements from test 2 at LWC = 39 g/m^3.

that increasing LWC generally resulted in some increase in δ_f and increasing θ generally resulted in a decrease in δ_f values on both the upper and lower surfaces.

Thickness measurements from test 2 are shown for the clean model wing in Figs. 9 and 10. Figure 9 shows the effect of increasing LWC at $\alpha = 4$ deg and Fig. 10 the effect of increasing α at LWC = 39 g/m^3. With the exception of the data on the lower surfaces at $x/c = 50.4\%$ (where continuous film breakdown may be occurring), the δ_f values are nearly the same for all LWC and α conditions. This result differs from test 1 and is most likely due to the differences in the section geometry and drop size distribution.

The data in Figs. 9 and 10 also show that the continuous film on the upper surface was quite thin (never greater than 2 mil) with the largest value at about $x/c = 35\%$. On the lower surface, the water film was considerably thicker at x/c aft of about 30%. At $x/c = 40\%$ for example, the δ_f on the lower surface was about 5 mil. In several respects, the δ_f data from test 2 show the same trends as test 1 (Fig. 8). In general, all of the clean wing measurements show that the continuous film was very thin on the upper surface, was thicker on the lower surface, and that the point of maximum thickness was further aft on the lower surface.

To better understand the film depths measured in test 2, the thickness δ of the natural boundary layer (without water spray) was calculated[4] for the model wing with the 64-210 section at $\alpha = 4$ deg. The results plotted in Fig. 11 show that the natural boundary layer is turbulent over virtually the entire upper surface and is laminar on the lower surface as far aft as $x/c = 64\%$. On the upper surface, the ratio of δ_f to δ at $x/c = 30\%$ is about 1% (2/200 mil). On the lower surface, δ_f is a much larger percentage of δ because of the larger water

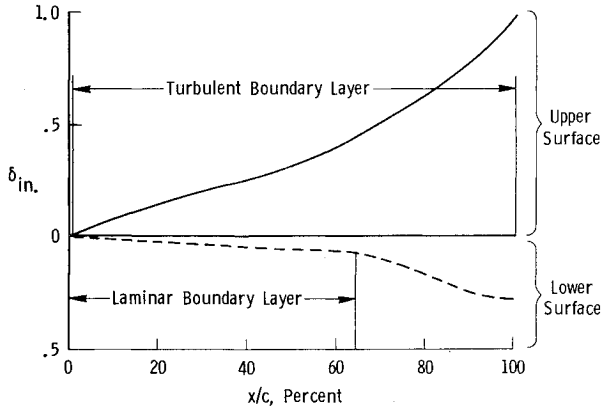

Fig. 11 Calculated boundary-layer thickness for clean wing (NACA 64-210 section, $c = 2.5$ ft, $\alpha = 4$ deg, $R_c = 3.9 \times 10^6$).

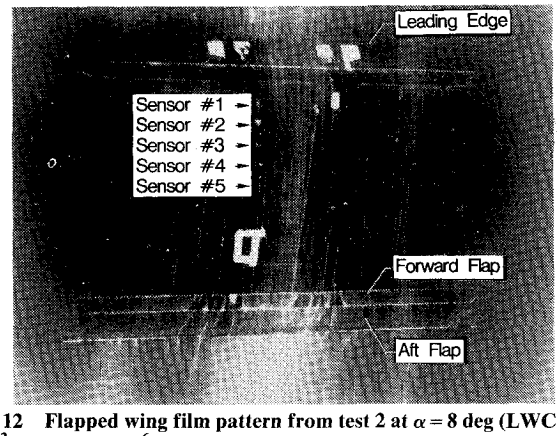

Fig. 12 Flapped wing film pattern from test 2 at $\alpha = 8$ deg (LWC = 20 g/m^3, $R_c = 2.5 \times 10^6$).

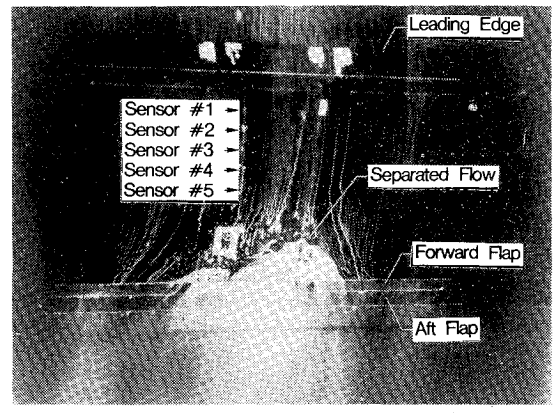

Fig. 13 Flapped wing film pattern from test 2 at $\alpha = 20$ deg (LWC = 20 g/m^3, $R_c = 2.5 \times 10^6$).

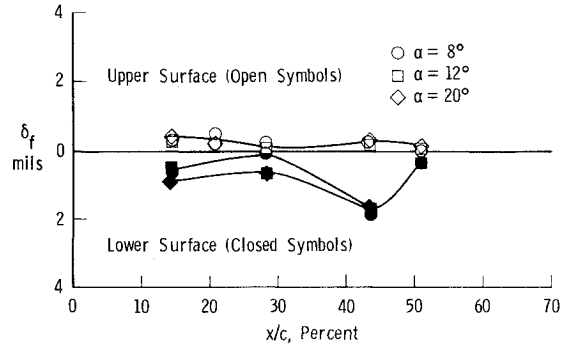

Fig. 14 Flapped wing film thickness measurements from test 2 at LWC = 20 g/m^3.

depth and the thinner laminar layer. (For $\delta_f = 5$ mil at $x/c = 40\%$, δ/δ_f is 10%.) The relatively large value of δ_f on the lower surface is significant because the boundary layer is laminar in this region and the calculated critical roughness height is only about 5 mil for this model wing at $x/c \simeq 35\%$.

The asymmetric shape of the continuous film measured in both tests would be expected on the basis of analytical studies.[5] These studies indicate that the asymmetry is an effect of the droplet impingement characteristics. Droplet trajectory calculations for NACA 65_1-208 and 65_1-212 wing sections at $\alpha = 4$ deg show that droplet impingement extends much further aft on the lower surface and that the impingement efficiencies are greater on this surface.

A preliminary evaluation of all of the clean wing results (Figs. 5-10) indicates that, for the clean wing models, detrimental changes in lift and/or drag are more likely to result from surface water on the aft, upper surface than from the continuous film on the forward section. Figures 5-7 indicate irregular surface patterns aft of midchord and evidence of separated flow at $\alpha = 14$ deg. Although the available data are insufficient to allow this surface roughness to be accurately modeled, it is suspected that this additional roughness may result in increased skin friction drag[6,7] and premature turbulent boundary-layer separation in the adverse presure gradient. Also, as noted earlier (Fig. 11), the boundary layer on the lower wing surface is largely laminar and early transition due to surface water is another probable source of decreased wing performance.[3,8]

Wings with Flaps

In test 2, data were obtained for the model wing with slats and flaps extended (Fig. 4). Photographs of the upper surface of this model in simulated rain at LWC = 20 g/m^3 and $\alpha = 8$ and 20 deg are shown in Figs. 12 and 13, respectively. For consistency, the photographs are shown for LWC = 20 g/m^3, although those at higher LWC show the same result. Unlike those of the wing without flaps, none of these photographs show significant water on the forward surface. At $\alpha = 8$ deg, some water is evident near the trailing-edge flaps. However, at $\alpha = 20$ deg, there appears to be a large separated flow area near the trailing-edge flaps as well as a great deal of water collected in and around the flap gaps.

Data from the thickness measuring sensors are shown in Fig. 14 for LWC = 20 g/m^3 and at $\alpha = 8$, 12, and 20 deg. The data (and other data not shown) indicate that the continuous film on both surfaces was relatively independent of α and was thinner on the flapped wing model than on the clean wing models. On the upper surface, δ_f never exceeded 1 mil and, on the lower surface, it never exceeded 2 mil. As in the case of the clean wing model, the maximum film depth on the lower surface was further aft than on the upper surface.

The decrease in δ_f on the upper surface of this configuration may be also explained by droplet trajectory analyses.[9] These data show that for a clean NACA 0012 wing section increasing α results in a decrease in the impingement efficiency on the upper surface. Increasing circulation by defecting flaps and slats would be expected to have the same effect. The decrease in δ_f on the forward part of the lower surface is probably due to the influence of the leading slat in catching and deflecting approaching droplets.

Evaluation of the data available for the flapped wing model (Figs. 12-14) indicate that the most probable causes of performance decrements due to simulated rain result from water in and around the flap gaps at large angles of attack. Wind tunnel data[10,11] show that the lift and drag of flapped wings are sensitive to the geometry of flap gaps. Surface water flowing from the lower to the upper surface through these gaps could

change this geometry and the associated lift and drag characteristics. Also, as with the clean wing, the presence of water roughness in an adverse pressure gradient on the aft upper surface may trigger local flow separation there.

This paper has not included consideration of scale effects on these model test results. These effects are discussed in detail in Ref. 12.

Summary

Surface water characteristics were observed and measured on two-dimensional model wings during two wind tunnel tests with simulated heavy rain. The wing chord lengths were 1.0 and 2.5 ft and the models were tested with and without leading-edge slats and trailing-edge flaps.

In the simulated heavy rain, the two clean wing models developed similar patterns. A continuous sheet of water extended to approximately the midchord of the upper and lower surfaces. On the NACA 64-210 section, the film depth on the upper surface was about 2 mil (1% of the natural boundary-layer thickness) at the 30% chord. On the lower surface, the maximum film depth was further aft and had a value of about 5 mil (10% of the natural boundary-layer thickness) at the 40% chord. At about midchord, the continuous sheet on the upper surface broke down into irregular surface patterns. At 0 deg angle of attack, individual runoff streams extended aft to the trailing edge and, at 14 deg angle of attack, large regions of water puddling indicating separated flow were observed on the aft portion of the upper surface.

The water film patterns on the model wing with flaps were significantly different from those of the model without flaps. The depth of water on the forward part of the airfoil was less and very little runoff water was visible on the aft upper surface. At $\alpha = 8$ deg, some water was evident on the upper surface near the trailing-edge flaps. At $\alpha = 20$ deg, however, a large separated area was observed on the upper surface near the flaps and a great deal of water was observed in and around the flap gaps.

These results indicate several possible causes of performance losses for model wings. In the clean configuration, surface water may contaminate the lower surface enough to cause early boundary-layer transition and an associated increase in drag. At high angles of attack, surface water collected on the upper surface near the trailing edge may trigger flow separation and an associated decrease in the lift/drag ratio.

The test of the model wing with slats and flaps indicates that, at angles of attack near 20 deg, surface water on the aft portion of the upper surface may again trigger separation, as noted above. In addition, water in and around the flap gaps may change the gap geometry with resulting adverse effects on lift.

References

[1]Hastings, E. C. Jr. and Weinstein, L. M., "Preliminary Indications of Water Film Distribution and Thickness on an Airfoil in a Water Spray," NASA TM 85796, 1984.

[2]Dunham, R. E. Jr., Bezos, G. M., Gentry, G. L., and Melson, E. Jr., "Two-Dimensional Wind Tunnel Tests of a Transport-Type Airfoil in a Water Spray," AIAA Paper 85-0258, Jan. 1985.

[3]Hansman, R. J. Jr. and Barsotti, M. F., "The Aerodynamic Effect of Surface Wetting Characteristics on a Laminar Flow Airfoil in Simulated Heavy Rain," AIAA Paper 85-0260, Jan. 1985.

[4]Stevens, W. A., Goradia, S. H., and Braden, J. A., "Mathematical Model for Two-Dimensional Multi-Component Airfoils in Viscous Flow," NASA CR-1843, 1971.

[5]Brun, R. J., Gallagher, H. M., and Vogt, D. E., "Impingement of Water Droplets on NACA 65_1 208 and 65_1-212 Airfoils at 4° Angle of Attack," NACA TN-2952, 1953.

[6]Young, A. D., Paterson, J. H., and Jones, J. L., "Aircraft Excrescence Drag," AGARD-AG-264, July 1981.

[7]Taylor, R. P., Coleman, H. W., and Hodge, B. K., "A Discrete Element Prediction Approach for Turbulent Flow over Rough Surfaces," Mississippi State University, State College, Rept. TFD-84-1, Feb. 1984.

[8]Holmes, B. J., Obara, C. J., and Yip, L. P., "Natural Laminar Flow Experiments on Modern Airplane Surfaces," NASA TP-2256, June 1984.

[9]Bragg, M. B., Gregorek, G. M., and Shaw, R. J., "An Analytical Approach to Airfoil Icing," AIAA Paper 81-0403, Jan. 1981.

[10]Riebe, J. M. and McLeod, R. G., "Low-Speed Wind-Tunnel Test of a Thin 60° Delta Wing With Double-Slotted, Plain, and Split Flaps," NACA RM L52J29, 1953.

[11]Riebe, J. M., "A Correlation of Two-Dimensional Data on Lift Coefficient Available With Blowing-, Suction-, Slotted-, and Plain-Flap High-Lift Devices," NACA RM L55D29a, 1955.

[12]Bilanin, A. J., "Scaling Laws for Testing of High Lift Airfoils under Heavy Rainfall," AIAA Paper 85-0257, Jan. 1985.